Available online at www.sciencedirect.com

ScienceDirect

Transportation Research Procedia 70 (2023) 299–306

Transportation Research Procedia

www.elsevier.com/locate/procedia

8th International Electric Vehicle Conference (EVC 2023)

# 12 Pulse High power Active Rectifier for Electric Vehicle Charging

Mohamad Taha[a]*, Ali Almaktoof [b], MTE Khan[b]

[a]*Electrical and Computer Engineering Department, Rafik Hariri University, P.O.Box 10 Damour-Chouf 2010, , Lebanon*
[b]*Electrical, Electronic and Computer Engineering Department, Cape Peninsula University of Technology Symphony Way, Cape Town, 7535, South Africa*

**Abstract**

The car industry pushes very fast toward electric vehicles (EVs). AC to DC charging stations pose big challenges for the power grid due to the heavy stress caused by electric-powered vehicles, especially when many vehicles are loading their accumulators simultaneously. The commercial success of electric vehicles (EVs) relies heavily on the presence of high-efficiency charging stations with low harmonics and a good power factor. To improve the power factor and boost the output voltage, this paper presents an analysis study and a simulation model of a 12-pulse high-power AC/DC active rectifier for EV charging stations. This converter topology provides bidirectional power flow and plays a double role as an AC to DC converter for power factor correction and as a DC converter for output regulation. The converter circuit is simulated using PSIM software, and results have observed. The simulation results for different conditions of operation are presented to highlight the feasibility and advantages of the proposed active rectifier.



*Keywords:* EVs, 12 pulse rectifier, Active rectifier, Vector control, Power factor, THD

## 1. Introduction

In modern transportation, the electric vehicle (EV) industry is growing very fast and is becoming one of the most important issues in modern technology and the power sector due to its zero emissions and pollution. EVs integration into power grids adds more challenges for power system operators. It is essential to evaluate potential grid impacts due to EV integration to guarantee standard-compliant grid operation (Rajendran et al. 2020). There are three levels of EV charging: level 1, level 2, and level 3, as outlined and explained by The Society of Automotive Engineers. Each level relates to its power and charging time (Carmen et al. 2014; Kurczewski 2022).

Level 1: Automakers often include Level 1 charging equipment with new electric cars. This device plugs into a

* Corresponding author. Tel.: *+961-375-9994*; fax: *+961-560-1830*.
*E-mail address:* tahamh@rhu.edu.lb


10.1016/j.trpro.2023.11.033

typical household 120-volt outlet. This type of charging replenishes your car's battery pack at a very slow rate and takes a very long time to be fully charged.

Level 2: Level 2 charging operates at 240 volts and typically at three to four times the amperage of a lesser Level 1. The majority of Level 2 units add electricity to your EV's battery pack at a rate that's roughly six to eight times faster than Level 1 setups, equating to 12–32 miles of driving range for each hour of charging.

Level 3 or DC Fast-Charging: Level 3 chargers are the faster chargers for EVs. Alternatively known as DC fast chargers, Level 3 chargers are especially useful during long trips that necessitate charging between destinations, as this sort of charging can add around 100–250 miles of range in 30–45 minutes. Unlike Level 1 and Level 2 charging setups, Level 3 setups connect to the vehicle by way of a socket with additional pins for handling the higher voltage (typically 400 or 1000 volts). Level 3 charge rates currently range from as little as 50 kW to as high as 350 kW. Level 3 chargers are usually located in charging stations with high-power AC to DC converters. Fig. 1 shows the general block diagram for a level 3 charger, which consists of three stages, namely the input filter, AC-DC rectifier, and DC-DC converter stages. Table 1 shows the specifications of electric vehicle chargers (Dusmez et al. 2011).

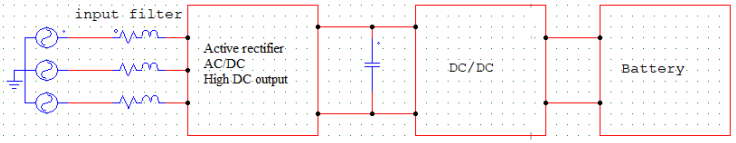


Fig. 1. Level 3 charger.

Table 1. Specifications of Electric Vehicle Chargers

| | AC Voltage (V) | Max. Current (A) | Max. Power (kW) |
|---|---|---|---|
| **Level 1** | 120 | 16 | 1.92 |
| **Level 2** | 240 | 80 | 19.2 |
| **Level 3** | 300-600 | 400 | 240 |

In EVs, the power electronics segment plays a very important role in controlling energy and improving power quality. EVs have been significantly enhanced to allow for a long driving range using novel battery technologies and fast-charging stations. The growth of the EV market has led to the significant issue of coming up with novel and innovative ideas to charge them (Dusmez et al. 2011; Kesler & Tolbert 2011; Xu & Chung 2016). Converters are considered nonlinear loads and, when connected to the grid, may inject some harmonics and disturb the whole grid system. There are many standards to limit and enforce the harmonics, and this should apply to any converter topology design. There are many types of converter topologies available for EV charging, such as unidirectional boost converters, active boost or buck rectifiers, Swiss rectifiers, matrix converters, and Vienna rectifiers. The conventional 12-pulse rectifier using a diode bridge is one of the simplest converters since it does not require any control loop; however, this type of converter has a fixed DC output with high THD in the input current compared with the proposed 12-pulse active rectifier, which has the ability to stabilize variable output voltage. Using a decoupling feed-forward control method by DQ frame technique, the magnitude and phase of the input current can be controlled, and hence the power transfer that occurs between the AC and DC sides can also be controlled. The design of the system poses significant challenges due to the nature of the load range and requires many features, such as (Sangeeta & Shailaja 2012; Taha 2007):

- A high input power factor must be achieved to minimize reactive power requirements.
- Power density must be maximized for a minimum size and weight.
- Regulated DC voltage.
- Sinusoidal and low harmonic contents on supply current.

## 2. Harmonics and power factors for an uncontrolled diode rectifier

Nonlinear loads, such as rectifiers, can cause harmonics on the grid systems, which will increase losses and can excite resonance in some circuits, resulting in elevated voltages. In general, rectifiers produce harmonics in the following order:

$$h = \frac{f_h}{f_1} = K.P \pm 1 \quad (1)$$

Where: $h$ = order of harmonics; $f_h$ = frequency of the harmonic current; $f_1$ = fundamental frequency; $P$ = rectifier pulse number; and $K$ = 1, 2, 3, ...

If the voltage or current waveforms contain harmonics, the phase angle between them no longer represents the value of the power factor. In general, the power factor could be calculated as (Taha 2007).

$$P\,F = \frac{\text{mean power}}{V_{rms}I_{rms}} \quad (2)$$

Rectifiers draw non-sinusoidal current and have high harmonic components; however, if the input voltage of the rectifier is considered to be sinusoidal, it is well known that the power factor and current THD for a 6-pulse diode rectifier are equal to 0.955 and 31.08%, respectively. Although the power factor is good, the THD value is relatively high and could have a bad effect on the grid. A 12-pulse diode rectifier is fed from a three-phase star-connected transformer on the primary side and star and delta transformers on the secondary side. Each transformer on the secondary side feeds a three-phase, six-pulse rectifier, and they add together to form a 12-pulse rectifier. This configuration gives 30 degrees of phase shift, which gives perfect harmonic cancellation. The turn ratio of the delta transformer must be multiplied by factor in order to get the same voltage level, In a three-phase, six-pulse rectifier, the dominated harmonics are the $5^{th}$ and $7^{th}$. With a 12-pulse arrangement, the $5^{th}$ and $7^{th}$ harmonics are cancelled. The THD for a 12-pulse rectifier equals 15.5%, which is reduced by 50 % compared with a 6-pulse rectifier.

## 3. Harmonics and power factors for an uncontrolled diode rectifier

A 12-pulse active rectifier could be used for level 3 EV chargers, which give very low THD and unity power factor; this is shown in Fig. 2. Many advantages are associated with this type of rectifier:

- The power factor can be controlled by using DQ vector control.
- THD is very low.
- Bidirectional power flow
- Boosting and regulating DC voltage

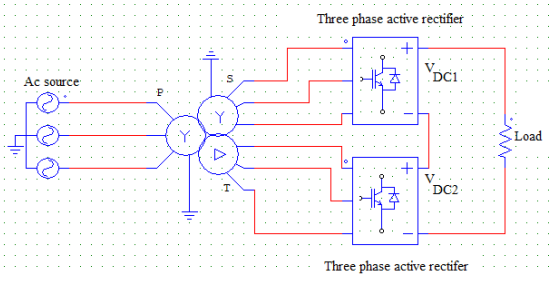


Fig. 2. AC to DC 12 active rectifier

Fig. 3 shows a single 6-pulse active rectifier configuration. The DQ transform, usually called the Park transform, is a space vector transformation of the instantaneous three-phase voltages and currents from a stationary phase coordinate system (ABC) to a rotating coordinate system (DQ). The general formulas for DQ transformations are

given as follows: We assume that the three-phase source voltages $v_a$, $v_b$, and $v_c$ are balanced and sinusoidal with an angular frequency ω.

The components of the input voltage phasor along the axes of a stationary orthogonal reference frame (α, β) are given by (Taha 2007):

$$V_\alpha = \frac{2}{3}V_a - \frac{1}{3}V_b - \frac{1}{3}V_c \quad (3)$$

$$V_\beta = \frac{1}{\sqrt{3}}V_c - \frac{1}{\sqrt{3}}V_b \quad (4)$$

The input voltage can then be transformed to a rotating reference frame DQ chosen with the D axis aligned with the voltage phasor. The voltage components are given by:

$$v_d = V_\alpha \cos \omega t - V_\beta \sin \omega t \quad (5)$$

$$v_q = V_\alpha \sin \omega t + V_\beta \cos \omega t \quad (6)$$

The same transformations are applied to the phase currents:

$$i_d = I_\alpha \cos \omega t - I_\beta \sin \omega t \quad (7)$$

$$i_q = I_\alpha \sin \omega t + I_\beta \cos \omega t \quad (8)$$

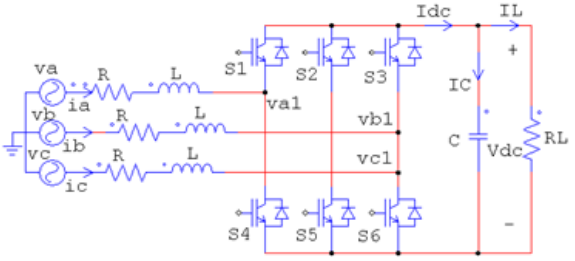


Fig. 3. 6 pulse Active Rectifier configuration.

Let $v_{a1}$, $v_{b1}$ and $v_{c1}$ be the fundamental voltages per phase at the input of the converter.

$$v_a = Ri_a + L\, di_a/dt + v_{a1} \quad (9)$$

$$v_b = Ri_b + L\, di_b/dt + v_{b1} \quad (10)$$

$$v_c = Ri_c + L\, di_c/dt + v_{c1} \quad (11)$$

Where L and R are the values of input line inductance and input resistance, respectively.

Taking the DQ transformation for the inductor, the input voltage to the converter in the DQ reference frame given by:

$$v_d = Ri_d + L.di_d/dt - \omega Li_q + v_{d1} \quad (12)$$

$$v_q = Ri_q + L.di_q/dt + \omega Li_d + v_{q1} \quad (13)$$

Note that $v_{d1}$ and $v_{q1}$ are the DQ components at the converter terminals.

The instantaneous active and reactive powers are given by:

$$P_d(t) = 3/2\,(v_d.i_d + v_q i_q) \quad (14)$$

$$Q_d(t) = 3/2\,(v_d.i_q + v_q i_d) \quad (15)$$

During the steady state and by assuming the converter losses are negligible, the DC and AC power are equal, therefore:

$$P_d = P_{DC} = V_{DC}.I_{DC} \quad (16)$$

$$I_{DC} = \frac{P_d}{V_{DC}} = \frac{3\,(vd.id + vqiq)}{2V_{DC}} \tag{17}$$

For a power balance, the delivering power should equal the absorbing power therefore:

$$P_{AC} + P_{DC} + P_C = 0 \tag{18}$$

where $P_C$ is the power in the capacitor filter.

If the synchronous frame is aligned to voltage, the quadrature component, $v_q = 0$. Therefore, the power equations reduce to:

$$P_d = 3/2\,(vd.i) \tag{19}$$
$$Q_d = 3/2\,(v_d.i_q) \tag{20}$$

Therefore: $I_{DC} = \frac{P_d}{V_{DC}} = \frac{3\,(vd.id)}{2V_{DC}}$ (21)

That gives:

$$P_{AC} + P_{DC} + P_C = 3/2\, v_d.i_d + V_{DC}.I_{DC} + V_{DC}.i_C = 0 \tag{22}$$

Therefore from equation (22), the capacitor current, is:

$$i_C = -\left(\frac{3\,(vd.id)}{2VDC} + I_{DC}\right) = C\frac{dV_{DC}}{dt} \tag{23}$$

Therefore: $\frac{dV_{DC}}{dt} = \frac{i_C}{C} = \frac{-1}{C}\left(\frac{3\,(Vd.id}{2V_{DC}} + I_{DC}\right)$ (24)

From equation (24) by controlling the active current $i_d$, the DC output voltage of the rectifier can be controlled. Fig. 4 shows the schematic of the DQ control scheme implemented in the input converter. Inverse DQ transformations then need to be applied to provide the three phase modulating waves ($v_{aref}$, vbref, and $v_{cref}$) for the PWM generation. DQ vector control has several benefits, such as easy control of reactive and active power and a very fast dynamic response in the current loop.

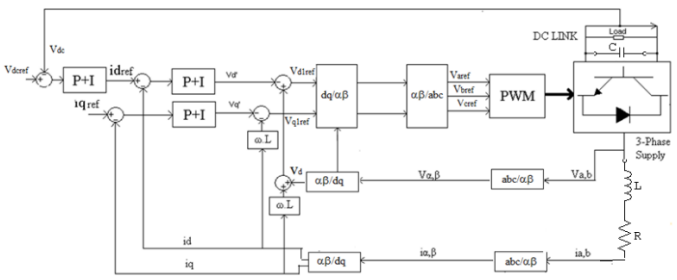


Fig. 4. DQ control for the input converter

The proposed control scheme consists of two parts (Taha 2007) an outer voltage controller and an inner current controller. The outer voltage controller regulates the DC link voltage. The error signal is used as input for the PI voltage controller, which provides a reference to the D current of the inner current controller. Fig. 5 shows the close loop control of the outer voltage control. The relationship between the DC voltage, the D axis input voltage and the modulation M index is given by:

$$V_{DC} = \frac{2\sqrt{2}V_d}{M} \text{ or } \quad M = \frac{2\sqrt{2}V_d}{V_{DC}} \tag{25}$$

$$I_{DC} = \frac{3}{2\sqrt{2}} M\, I_d \tag{26}$$

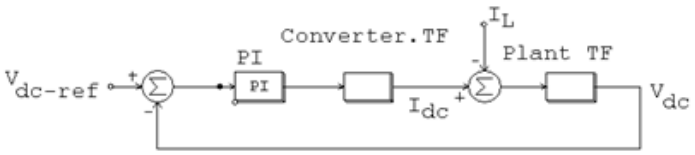


Fig. 5. Close loop control of outer dc voltage control.

The transfer function for each block is: PI TF : $K_p + K_i \frac{1}{S} = K_P(\frac{S+a_i}{S})$, Converter TF: $\frac{3}{2\sqrt{2}}M$ and Plant TF: $\frac{1}{CS}$
Therefore, the characteristic equation for the DC link voltage control is given by:

$$S^2 + \frac{3MK_p}{2\sqrt{2}C}S + \frac{3MK_pa_i}{2\sqrt{2}C} = 0 \quad (27)$$

General equation for second order characteristic equation is given by:

$$S^2 + 2\,\xi\omega_n\,S + \omega_n^2 = 0 \quad (28)$$

Therefore, the controller parameters are given by:

$$K_p = \frac{4\sqrt{2}\,C\xi\omega_n}{3M} \quad \text{and } a_i = \frac{2\sqrt{2}C\,\omega_n^2}{3MKp}$$

Fig. 6 shows the close loop control of the inner current control. A PI Inner DQ current control refers the phase current measurements to a rotating coordinate frame DQ fixed to the supply voltage. If the phase currents are in phase with the supply voltages, the current referred to the direct D axis becomes the DC link current, and the current referred to the quadrature Q axis is equal to zero. Figure 6. Close loop control of inner current control. The coordinate transformation is done by using phase angle information derived from the measurement of the supply voltages. However, if the system needs to operate with a leading or lagging power factor, the Q axis reference value can be changed to define the displacement angle of the rectifier. The final demand voltages are transferred back into stationary coordinates, and the resulting sinusoids are used to generate the PWM.

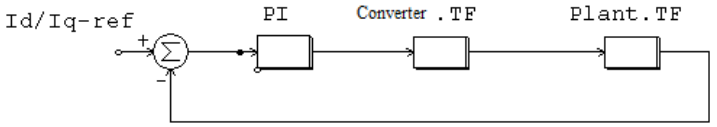


Fig. 6. Close loop control of inner current control

Plant TF = $\frac{1}{R+LS}$ , and the converter may be modelled as a first order lag. = $\frac{1}{1+TS}$ , where $T = \frac{1}{F_s}$, $F_s$ is the switching frequency. The same procedure can be used to calculate the parameters of the controller. Simulink or other tools can be easily used to tune the PI controller by using Zeigler-Nichol's method.

## 4. Simulation results

In order to optimize the power quality and transient behaviour of the power distribution system, a well-designed simulation model of the 12-pulse active rectifier based on detailed component models will be necessary. For high voltage demand, the two rectifiers are connected in series, and for high current demand, the rectifiers may connect in parallel. The converter has been simulated for various operating conditions with the following parameters: Furthermore, the turn ratio of the transformer can be changed to reduce the input AC voltage for each active rectifier. Input inductance is 500 H, and input resistance is 0.1 Ω. For each converter. DC filter C = 500 F. For each converter. Switching frequency is 5 KHz. AC input voltage is 220 V RMS. Resistive load = 30 Ω. The DC voltage reference for each converter is set to 800V.

Simulation results (from Fig. 7 to Fig. 12) are very encouraging and show that, compared with a conventional 12-

pulse diode rectifier, the low-order harmonics are totally eliminated, and only very low harmonics around the switching frequency at frequencies $f = mf_s$ where $m = 1, 2, \ldots+\infty$

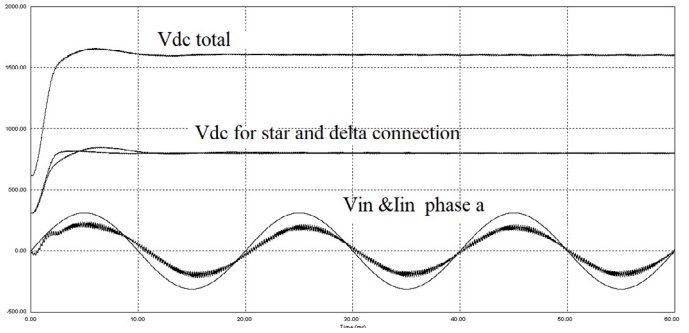


Fig. 7. DC voltage and input voltage and current at unity PF

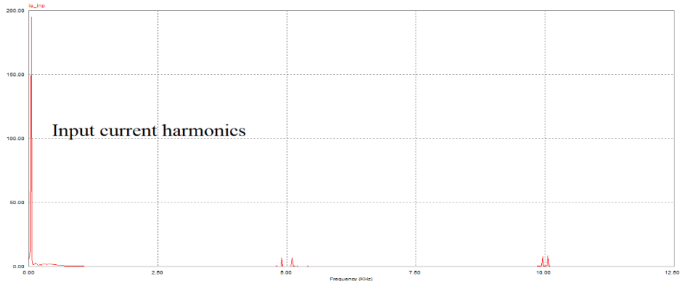


Fig. 8. Input current harmonics.

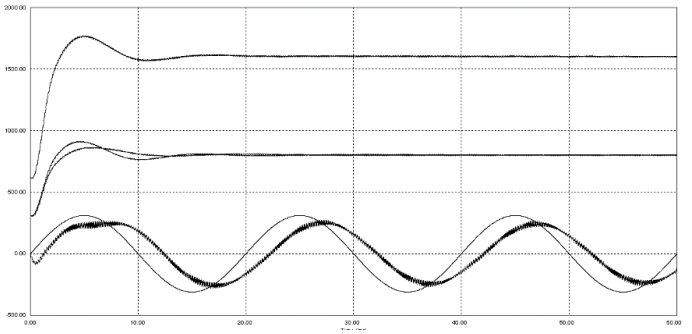

Fig. 9. DC voltage and input voltage and current lagging PF

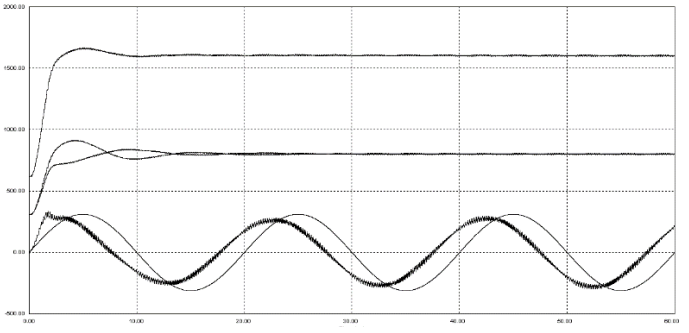

Fig. 10. DC voltage and input voltage and current leading PF

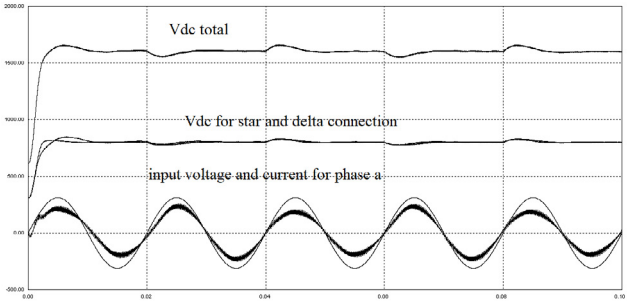


Fig. 11. DC voltage and input voltage and current 25% load changing

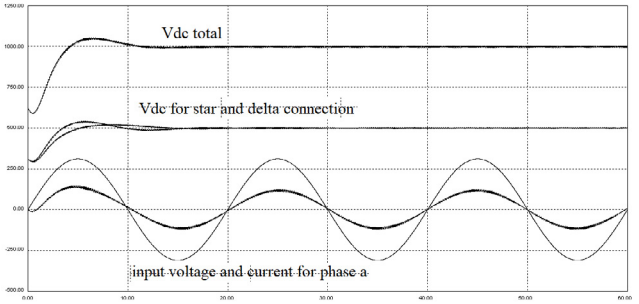


Fig. 12. DC voltage and input voltage and current (changing turn ratio 2/1)

## 5. Conclusion

With the future use of advanced power electronics, a 12-pulse active rectifier gives a very beneficial approach within EV charging stations. Low-frequency current harmonics can be eliminated, and there is the possibility to operate the rectifier at a variable power factor in order to provide system-level benefits. and keeping the input current harmonics low.

## Acknowledgements

Authors wish to acknowledge support and encouragement from Rafik Hariri University - Lebanon and Cape Peninsula University of Technology- South Africa.

## References

Carmen Falvo M, Sbordone D, Bayram S and Devetsikiotis M 2014 EV Charging Stations and conference paper, International Standards.

Dusmez S, Cook and Khaligh A 2011 Comprehensive Analysis of High Quality Power Converters for Level 3 Off-board Chargers IEEE Vehicle Power and Propulsion Conference.

Kesler M, Kisacikoglu MC and Tolbert LM 2011 Vehicle-to-grid reacative power operation using plug-in electric vehicle bidirectional ofboard charger. IEEE Trans Ind Electron 61:6778–6784.

Kurczewski N 2022 Different levels of EV Charging Car and drive magazine.

Rajendran G, et al. 2020 Energy-efficient converters for electric vehicle charging stations Published online: 9 March 2020 © Springer Nature Switzerland AG 2020.

Sangeeta Sarali D and Shailaja P 2012 *Mitigation* Of. Harmonics Using Thyristor Based 12 Pulse. Voltage Source PWM Rectifier. In: IJRET Volume 1 Issue 3.

Taha MH, 2007. Active rectifier using DQ vector control for aircraft power system 2007. IEMDC.

Xu NZ and Chung CY 2016 Reliability evaluation of distribution systems including vehicle-to-home and vehicle-to-grid. IEEE Trans Power Syst 31:759–768.